The Effect of Environmental Conditions on the Electrical Performance of Polypyrrole.

Anton Terpstra

June 20, 2024

Course: Bachelor Research Project [WBCE901-15]
Student number: S4897056
First Supervisor: Prof. R.K. Bose
Second Supervisor: Prof. F. Picchioni

university of groningen

1 Abstract

Polypyrrole (PPy) is a conductive polymer that has gained significant attention for its high conductivity, environmental stability, and biocompatibility. In recent decades, extensive research and application development have been conducted. This study investigates the effects of environmental conditions on the performance of oCVD polypyrrole thin films. The influence of pH and electrolyte solutions on the properties of polypyrrole thin films is highlighted, as the focus lies on the application as pH sensors and as a supercapacitor material. UV-vis spectroscopy revealed that the optical band gap of PPy films increases with pH due to deprotonation, leading to a lower concentration of bipolarons and polarons. Additionally, it was found that thicker films exhibit lower optical band gap due to having less surface imperfections. Furthermore, a reaction ratio of 0.2 was found to be the most favourable to avoid underdoping or overoxidation. For pH sensors, the ideal parameters were found to be a thin film ($\tilde{1}$00nm) with a reaction ratio of 0.2. To investigate the performance of PPy as a supercapacitor material, the electrolyte solutions, reactor position and nitrogen patch flow were varied. Profilometry depicted that an increasing nitrogen patch flow was suspected to initially act as a diluent and then acts as a carrying agent. Furthermore, contact angle measurements demonstrated that electrolyte treatments influenced wetting properties, with KCl and HCl treatments showing similar behaviour, while KOH treatment resulted in decreased contact angles attributed to increased surface roughness. Four-point probe conductivity measurements revealed varying trends among electrolyte-treated samples, with KCl and HCl-treated samples exhibiting lower conductivity in row 3, possibly due to the introduction of Cl^- ions causing overoxidation. Furthermore, in row 2 an increase in conductivity was observed. This was attributed to the dedoping of the over-oxidized samples. KOH-treated samples showed negligible conductivity, likely due to surface imperfections, delamination and cracks in the surface. This research showed that KOH is not a suitable electrolyte for PPy. Long-term stability studies indicated decreased band gap measurements over time, suggesting polarons to have rearranged to bipolarons over a longer duration. Moreover, swelling of the material could be a reason for the lower band gap values. Overall, this research provides insights into PPy film properties for applications as pH sensors and as a supercapacitor material. The importance of considering environmental impact, such as pH and electrolyte effects, was emphasized.

Contents

List of Figures

List of Tables

2 Introduction

Electrically conductive polymers represent an interesting type of material with unique electronic, optical, and electrochemical properties. Unlike traditional polymers, which are insulators, conducting polymers possess a conjugated backbone structure that allows for the delocalization of electrons along the polymer chain. This delocalization allows for electrical conductivity[1]. Moreover, these polymer materials combine the mechanical properties of polymers with the conductivity of metals or semiconductors. In fact, the structural rigidity of polymers compared to metals can be several orders of magnitude lower (200-210 GPa steel/1.1-2.0 GPa polyacetylene). Furthermore, conducting polymers are relatively lightweight and relatively cheap[2]–[4]. Some examples of conducting polymers include polythiophene (PTh), polyaniline (PANI), polyacetylene and polypyrrole (PPy). PPy is synthesized via the oxidative polymerization of pyrrole monomer. In this project, antimony pentachloride was used as the oxidant. Some other possible oxidants are iron trichloride, silver nitrate and ammonium persulfate[1],[5]. In the oxidative chemical vapour deposition (oCVD) process, the pyrrole monomer is vaporized and reacts with the oxidant in the gas phase. This technique offers several advantages over traditional solution-based methods. For example, it avoids the use of toxic solvents and associated side reactions, enabling the deposition of uniform, high-conductivity films on a wide variety of substrates, including those sensitive to solvents. Additionally, oCVD allows precise film thickness and composition control, making it a niche method for producing high-quality conducting polymers[2],[5]–[7].

PPy exhibits unique properties, such as high electrical conductivity, environmental stability and biocompatibility. This has led to extensive research and application development[4]. Applications of conducting polymers, such as polypyrrole, span various fields. They are used in electronic devices like organic light-emitting diodes (OLEDs), organic field-effect transistors (OFETs), and electrochromic displays due to their semiconducting properties[2]–[4],[7]–[9]. Additionally, they find applications in energy storage and conversion, such as batteries, supercapacitors, and fuel cells, owing to their high electrical conductivity[2],[4],[10]. In addition, PPy can be suitable for use in drug delivery, tissue engineering and biosensors, such as pH sensors. Furthermore, due to PPy being lightweight and bio-compatible, it is especially suitable for modern electronic devices intended for skin contact or wearable devices[2]–[4],[7]–[9].

The structure of polypyrrole is investigated to understand its high conductivity. Since a conjugated backbone alone can only achieve a limited amount of conductivity, an additional mechanism must be present. Besides the conjugated backbone, PPy is suspected of exhibiting three different complex structures that contribute to its high conductivity: the neutral complex, bipolaron, and polaron[2],[6],[11],[12]. These chemical structures are depicted in Figure 2b. The polaron and bipolaron structures enhance conductivity by achieving higher electron delocalization. In this thesis, chlorine ions are the dopant atoms, introducing extra electrons and acting as counter ions. This doping process leads to the formation of polaron structures. When two polaron structures rearrange, a bipolaron is formed. Bipolarons are the major charge carriers in PPy due to their charge characteristics. Polaron structures can shift over 50 monomer units by rearranging, resulting in high electron delocalization. Additionally, the polaron and bipolaron complexes create extra energy states within the band gap of PPy, lowering the overall band gap energy of the material[2],[3],[7],[11]. A schematic of the band gap transitions in PPy is shown in Figure 3, and these transitions are further elaborated upon later in this thesis. Moreover, conduction can occur through direct or indirect electron transitions, with indirect transitions requiring additional energy to account for momentum differences. According to the literature, PPy primarily exhibits direct transitions between these energy levels[7],[8],[13],[14].
.

In pH sensors, the change in pH can significantly affect the band gap of PPy, making it essential to understand how the polymer interacts with different pH environments to ensure accurate measurements[4],[9],[15],[16]. pH sensors are mainly used in the realm of wound care. However, pH sensors can also be used for other medical appliances, such as blood analysis, gastric monitoring and urine monitoring[4],[9]. In the realm of wound care, monitoring pH levels is critical as it provides valuable insights into the progress of wound healing and the potential presence of infection. Besides the environmental pH, film parameters, such as thickness, reaction ratio, and film homogeneity, can have a significant influence on the pH sensitivity[2]. Thus, they can affect the accuracy and reliability of pH sensors. This sensitivity to environmental conditions and film parameters underscores the importance of carefully considering these factors when developing PPy-based applications. The advantages of polypyrrole-based pH sensors for wound healing are their biocompatibility, lightweight, flexibility, and fast and relatively easy detection. By integrating polypyrrole pH sensors into wearable devices, a new type of intelligent wound care system emerges that improves the response time and care for wound healing[4],[9],[15],[16].

Similarly, in the domain of energy storage, the use of supercapacitors has great significance due to their rapid charge and discharge capabilities, making them ideal for applications requiring high power outputs. Polypyrrole has gained attention for its potential application in supercapacitors, owing to its remarkable conductivity and electrochemical properties[4],[10]. The environmental impact, such as the type of electrolyte solution used, is crucial in optimizing the performance of PPy in these applications. Changes in the electrolyte environment can

affect the electrochemical behaviour of PPy, influencing the efficiency and durability of supercapacitors[3],[4],[10],[17]. Therefore, optimizing the environmental conditions and film parameters of PPy is fundamental to enhance their functionality in both healthcare and energy storage applications. Understanding these interactions helps in designing more effective and durable PPy-based devices that can reliably perform in varying conditions.

2.1 Research Aim and Hypothesis

This research aims to investigate the environmental effects on oCVD polypyrrole thin films. In this research, the influence of pH on the optical band gap of polypyrrole and the effect of electrolyte choice on the wettability and conductivity of PPy thin films was investigated. To investigate these subjects, research questions were formulated. Firstly, the research investigates how pH influences the optical band gap of polypyrrole, and in what way thickness and reaction ratio affect the pH sensitivity. Additionally, it examines the effect of electrolyte choice on the conductivity of PPy thin films and how it impacts the material performance. Subsequently, the study addresses the importance of the long-term stability of PPy for the applications investigated.

This study hypothesises that the optical band gap of PPy will vary with changes in pH. The optical band gap energy of PPy is expected to increase with increasing pH, with variations influenced by factors such as thickness and stoichiometric ratio of oxidant to monomer (RR). Furthermore, the study hypothesizes that the choice of electrolyte will impact the conductivity of PPy thin films, with different electrolytes affecting the doping/dedoping processes and charge transport properties such as wetting. Over the long term, the pH solutions are expected to have significant effects on the band gap of oCVD PPy films. Since prolonged exposure to different pH environments can lead to chemical changes in the polymer structure. In acidic or basic conditions, the polymer may undergo doping or dedoping processes, potentially altering its electronic properties[3],[8].

By addressing these research questions, this study aims to contribute to the understanding of the behaviour of PPy in response to pH changes and electrolyte environments, thereby improving the development of pH sensors and supercapacitor materials. In addition, no extensive research was done previously on the influence of pH on the optical band gap of PPy. This could give additional insight into the mechanism of pH response. Lastly, the effect of nitrogen patch flow on the PPy film is an interesting parameter that has not yet been extensively researched.

3 Methods

3.1 Oxidative chemical vapour deposition

Oxidative chemical vapour deposition (oCVD) is a niche technique used for the synthesis of conducting polymers on various substrates. By utilizing gaseous phase reactants, oCVD avoids numerous challenges often associated with conventional solution-based polymerization processes, such as side reactions and the use of toxic solvents. In addition, many conducting polymers, such as polypyrrole are insoluble, due to their stiff conjugated backbone. Therefore, processibility after polymerization is low. The insolubility of PPy makes utilizing the gaseous phase a major advantage of oCVD over solution-based processes[5]. Moreover, this method facilitates the synthesis of homogeneous, thin films with higher electrical conductivity compared to solution-based polymerization due to several factors. It ensures uniform application and precise thickness control, reducing impurities and defects that typically arise from solvent residues. The process promotes better molecular alignment and higher degrees of crystallinity, which enhance charge carrier mobility. Additionally, it achieves a smoother interface with the substrate, minimizing scattering sites for charge carriers. By eliminating solvent-related issues and optimizing film structure and purity, this method significantly improves the electrical conductivity of the resulting thin films[2],[5]. Additionally, the absence of solvents in the process expands the range of substrate choices, as solution polymerization can cause substrates to dissolve or disintegrate. The oCVD was performed in a custom-built oCVD reactor (Figure 1)[6]. During oCVD, modifying various reaction parameters can alter the reaction and the deposited film, such as the thickness and doping concentration of the PPy film. The parameters affecting changes in the PPy film include the stoichiometric ratio of monomer to oxidant (reaction ratio, RR), nitrogen patch flow, pressure, deposition temperature, deposition time, and position in the reaction chamber[2],[5]–[7]. In this study, oCVD was employed to deposit PPy onto optical quartz substrates (Präzisions Glas & Optik GmbH, Germany, 15x10mm)[2]. Optical grade quartz was used as it is optically invisible for the UV-vis measurements that were done.

To evaluate the effect of pH on the optical band gap of oCVD PPy, thin coatings were deposited on quartz substrates. The samples were then immersed for two hours into buffer solutions (20ml) with increasing pH of 4, 7 and 10. In addition, some samples were evaluated in a range of 4-12 with pH increments of 1. The buffer solutions

were prepared by mixing standard buffers of pH 4, 7, and 10 in the appropriate ratios. Solvent abundance was used to ensure equilibriation, this was done to ensure the availability of counter ions. In order to evaluate the effect of reaction ratio on the pH response of oCVD PPy, samples with varying reaction ratios (RR 0.1, 0.2, 0.3) were prepared. The variations were then immersed for two hours into buffer solutions (20ml) with pH 4, 7 and 10 as mentioned previously. In addition, for RR 0.2 the solvation was done in a range of 4-12 with pH increments of 1. Furthermore, the effect of thickness on the optical band gap was investigated by varying the deposition time and thus the thickness of the substrates with RR 0.2. The thickness of the thin and thick samples were +/-100nm and +/-300nm respectively. The samples were similarly equilibrated in pH buffers (4, 7 and 10). Furthermore, the long-term effect of pH solutions on the PPy substrates was investigated by submerging the samples for five days with intermediate stirring. All oCVD reactions were performed with 30 sccm nitrogen flow. The parameters investigated in this study are summarized in Table 1. All the submerged samples were dried with Kimtech wipes after equilibriation. Subsequently, the samples were promptly measured with UV-vis spectroscopy and stored in a vacuum chamber.

The effect of electrolyte solutions on oCVD PPy films is explored by immersing the oCVD PPy samples in KOH, KCl, and HCl solutions (1M, 20ml) similarly for two hours. Additionally, the effect of nitrogen patch flow and the position within the oCVD reactor on the behaviour of electrolyte solutions is investigated. A schematic representation of the oCVD reactor is shown in Figure 1. The different reactor positions are depicted schematically in this figure. The nitrogen patch flow was varied in the range of 15-25 sccm and two reactor positions were evaluated (row 2 & 3). Essentially, by adjusting both the nitrogen patch flow and its position, the thickness was varied. The sample parameters are depicted in Table 1. In addition, samples were submerged for five days using all three electrolytes to investigate their long-term stability. The thickness of the oCVD PPy coatings was measured by profilometry while the electrical conductivity measurements were performed using a four-point probe. Furthermore, the surface energy of the oCVD PPy coated samples equilibrated in different electrolyte solutions were investigated by performing contact angle measurements.

$$\text{Reaction ratio(RR)} = \frac{\text{Oxidant flow rate (sccm)}}{\text{Monomer flow rate (sccm)}} \tag{1}$$

Sample Name	**RR***	**Deposition time (min)**	**Nitrogen flow (sccm)**	**Reactor position**
PPy-0.1thin	0.1	30	30	
PPy-0.2thin	0.2	30	30	
PPy-0.2Thick	0.2	60	30	
PPy-0.2thinN15	0.2	30	15	Row 3
PPy-0.2ThickN15	0.2	30	15	Row 2
PPy-0.2thinN20	0.2	30	20	Row 3
PPy-0.2ThickN20	0.2	30	20	Row 2
PPy-0.2thinN25	0.2	30	25	Row 3
PPy-0.2ThickN25	0.2	30	25	Row 2
PPy-0.3thin	0.3	30	30	

Table 1: Operational parameters for oCVD depositions of PPy. (*Equation 1)

3.2 UV-vis spectroscopy

UV-vis analysis measures the amount of light absorbed, scattered or transmitted by a sample at wavelengths in the ultra-violet and visible spectrum ranging from 190-1100 nm. This research uses an Agilent Cary 60 UV-Vis spectrophotometer[6]. For conducting polymers, UV-vis analysis provides critical information about the optical absorption transitions and the corresponding energy levels within the band gap (Figure 3). The absorption band positions and the intensity of the spectrum allow for detailed analysis of the doping and dedoping processes. Additionally, UV-vis can provide evidence and further information about the suggested charged complexes, such as polarons and bipolarons[2],[12],[13],[19].

Moreover, using the absorption spectroscopy, the optical band gap energy can be extracted by employing the Tauc equation. With Equation 2 we can plot the photon energy against $(\alpha \cdot h \cdot \nu)^{\gamma}$. Linear regression is applied to this plot, and by extrapolating this line to the x-axis, the intersection corresponds to the band gap energy of the material[20]. The band gap can be either direct ($\gamma = 2$) or indirect ($\gamma = 0.5$) depending on the momentum of

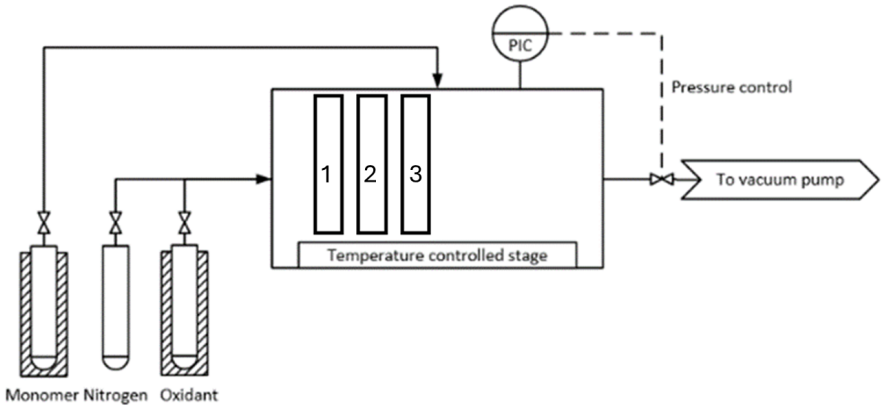

Figure 1: Schematic representation of the used oCVD reactor. Obtained from Hendriksen (Rug, 2021)[18].

the photon. For PPy, research has shown the transition to be direct, as the Tauc plots with indirect transition exhibited irregularities and the linear region was not present in some cases.[12],[13].

Tauc plots offer several advantages over other methods for estimating the optical band gap, such as photoluminescence spectroscopy, cyclic voltammetry, and impedance spectroscopy. Tauc plots provide a straightforward method for estimating the optical band gap, with the plotting and extrapolation process being relatively simple and not requiring complex calculations. However, Tauc plots also have some limitations. Firstly, the method assumes a specific type of optical transition (direct or indirect). Incorrect assumptions towards these transitions can lead to inaccurate band gap estimations. Moreover, the linear fit to the linear region can be subjective, and different interpretations can lead to variations in the calculated band gap. The accuracy heavily depends on the quality of the UV-vis data and the precision of the linear regression. Additionally, imperfections, inhomogeneities, and impurities in the sample can affect the absorption spectrum[20],[21].

$$\alpha(h\nu)^{\gamma} = B\,(h\nu - E_g) \tag{2}$$

where:

$\alpha(\nu)$ is the absorption coefficient (cm^{-1}),
h is the Planck constant (eVs),
ν is the photon energy (s^{-1}),
E_g is the band gap energy (eV)
B is a constant assumed to be 1 for amorphous polymers
γ is the Tauc exponent, 1/2 is an indirect and 2 is a direct transition.

3.3 Profilometry

Stylus profilometry is a surface technique used to measure surface topography, roughness, and step heights with high precision. It works based on the principle of tracing a sharp stylus across the surface of a sample. As the stylus moves along the surface, it measures the vertical displacement of the surface relative to a reference plane. The vertical movement of the stylus is typically detected using a piezoelectric sensor or optical interferometry, allowing precise measurement of surface features.[22]. A scratch is made on the surface of the thin PPy samples, exposing the underlying substrate. Utilizing this scratch, the thickness of the film is measured at various points. Over 15 measurements were conducted across the film to ensure a reliable approximation of its thickness.

3.4 Contact angle

The contact angle is a measure of the wetting behaviour of a liquid on a solid surface. It quantifies the degree of curvature of a liquid droplet at the solid-liquid interface. Wettability refers to the ability of a liquid to spread over a solid surface. It is influenced by properties such as surface tension, surface energy, and surface roughness of the solid material[23],[24]. For conducting polymers used as supercapacitors, achieving high wettability is essential for facilitating efficient ion transport between the electrolyte and the electrode surface[23]–[25]. In this research, drops (20 µL) of KOH, KCl and HCl were deposited on the PPy surface to measure the contact angle for these electrolytes.

3.5 Four-point probe conductivity

Four-point probe conductivity measurement is a technique used to determine the electrical conductivity of a surface. This method involves applying a known current through two outer probes while measuring the voltage drop across the material using two inner probes. By analyzing the voltage and current, the sheet resistance of the material can be calculated using Equation 3. To calculate the conductivity of the films, the sheet resistance (R) was measured with a four-point probe (Ossila Ltd, UK.) on PPy-coated glass slides. The results were averaged over at least 50 measurements at different locations on the same sample. The PPy film resistivity was then calculated by Equation 4 and Equation 5. All the variations were evaluated to test the influence of nitrogen patch flow on the behaviour of PPy in a supercapacitor[12],[26]. The four-point probe has some limitations that need to be considered. The probe measurement depth is limited to the near-surface region, which may not represent the entire film properties. UV-vis measurements are more reliable for assessing bulk properties. In addition, the method is highly sensitive to contamination, oxidation, and defects on the surface.

$$R_s = \frac{\pi}{\ln(2)} \cdot \frac{V}{I} \tag{3}$$

Where:

V = Voltage across outer probes (U)
I = Current through inner probes (A)

$$\rho = R \times t \tag{4}$$

Where:

R = Sheet Resistance (Ω/m^2)
t = Thickness (m)

$$\sigma = \frac{1}{\rho} \tag{5}$$

Where:

σ = Conductivity (S/m)
ρ = Resistivity (Ω/m)

4 Results and Discussion

4.1 Effect of pH on band gap transitions of oCVD PPy

The electrical conductivity of conjugated polymers such as PPy is significantly modulated by their doping concentration. Early studies by Kaufman et al. show that the pH can modulate the availability of dopant counter ions and thus the electric transitions[11]. In addition, it was summarized that in non-degenerate ground state polymers such as PPy, introducing defects, such as removing a single electron from the conjugated backbone through doping, accompanied by lattice relaxation generates a polaron. The polaron forms multiple optical transitions below the original conduction band (Figure 3). Further doping of PPy chains leads to the generation of more polarons that rearrange and recombine to form bipolarons (Figure 2b). Yakushi et al.[27] confirmed the coexistence of neutral conjugated sections alongside polaron/bipolaron states in doped PPy chains.

UV-vis spectroscopy was used to obtain the optical band gap and electronic band transitions in oCVD PPy films. Three major peaks were identified in the UV-vis spectra[19]. The UV-vis spectrum of oCVD PPy was depicted in Figure 2a. In addition, a schematic of the transitions is depicted in Figure 3. Edberg et al. described the band transition corresponding to each peak for PEDOT[12]. Kaufman et al. confirm the similarity with PPy[11]. According to them, peak 1 ($\tilde{4}$20nm) of Figure 2a corresponds to an excitation of the neutral polymer (transition 1), peak 2 ($\tilde{5}$00nm) is obtained from either a transition from the HOMO polaron level to the first band of the polaron level (transition 2) or from the HOMO level to the first bipolaron band (transition 4), peak 3 ($\tilde{6}$90nm) is related to excitation from the first polaron level to the second polaron level (transition 3). Moreover, peak 4 ($\tilde{9}$00nm) corresponds to excitation from the HOMO level to the second bipolaron or polaron band (transition 5). This information shows that peak 1 can be associated with the neutral PPy structure. In addition, Peaks 2–4 all involve transitions to, or between, polaron and bipolaron bands. Where peak 3 is associated with polarons and peak 4 is mainly associated with bipolarons. The peak and transition information was later used to support the band gap data.[12],[28],[29].

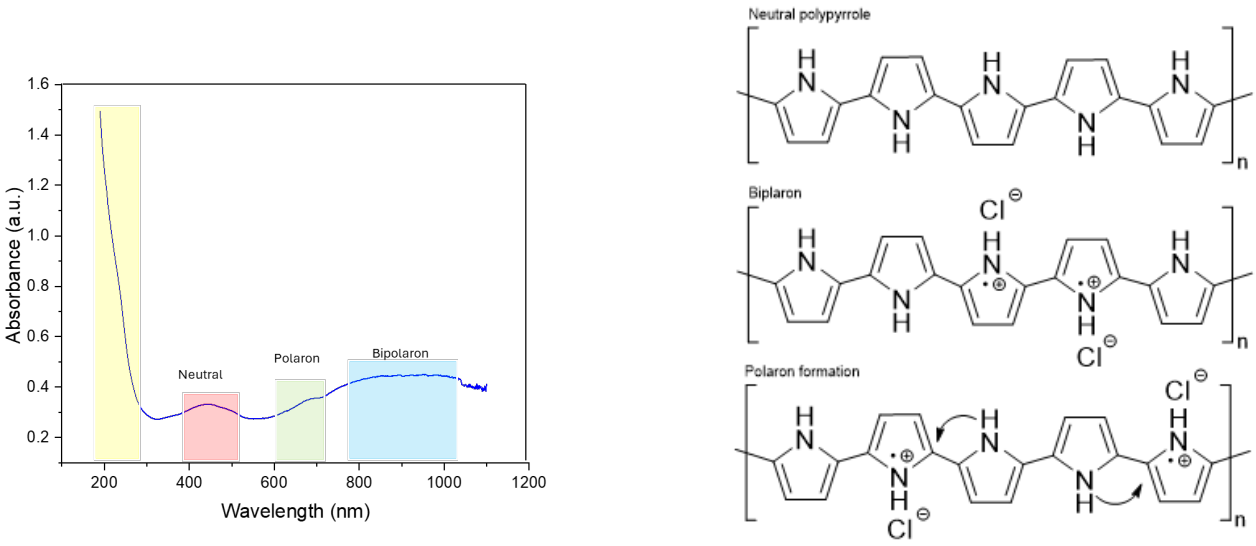

(a) UV-Vis spectrum of PPy measured between 190-1100nm

(b) Molecular structure of charged complexes

Figure 2: UV-Vis spectra and structure of PPy

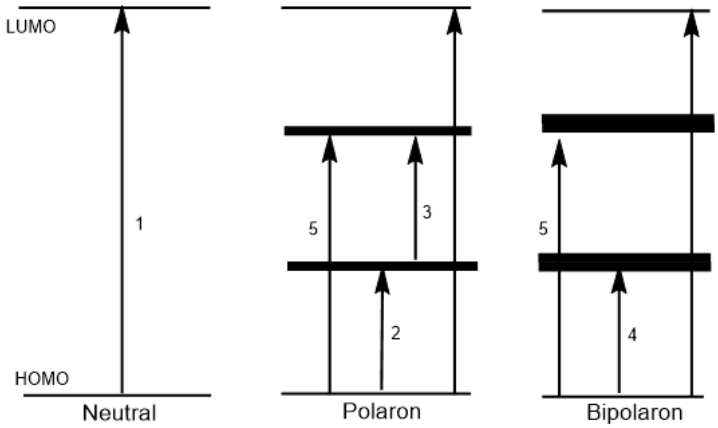

Figure 3: Depiction of the different energy state transitions in PPy.

To investigate the effect of pH on the band gap of oCVD PPy, the optical band gap was determined for pH 4-12 with increments of 1. The band gap energy is plotted against the pH of the equilibriating media in Figure 4b. The Tauc plots originating from the UV-vis measurements are depicted in Figure 16. An increase in band gap energy (5.09 to 5.38 eV) is observed with increasing pH. The increase in band gap is attributed to the deprotonation of the polaron and bipolaron complexes. As a result of the deprotonation, more neutral polypyrrole is present, thus increasing the overall band gap of the material[3],[9]. Forsyth et al.[30] report that the conductivity decreases with increased pH as a result of deprotonation. It is suggested that this deprotonated form of polypyrrole adopts an insulting structure. This can be attributed to the neutral PPy structure.

To further understand the mechanism of increased band gap, the UV-vis spectra were deconvoluted to depict the dominant transition. The deconvoluted spectra are depicted in Figure 4c, Figure 4d and Figure 18. By deconvolution, the polaron, bipolaron, combined and neutral peaks can be separated by fitting Gaussian curves. The peaks were previously assigned in Figure 2. At low pH a dominance of polarons is observed. Moreover, at high pH a shift of dominance to polarons is seen. This confirms the deprotonation mechanism[12].

Another effect observed when analyzing the UV-vis spectra was a blue shift with increasing pH. The UV-vis spectra of thin PPy RR 0.2, depicted in Figure 4a, show this phenomenon clearly. The blue shift is suspected to be caused by a decrease in conjugation length and the release of doping anions, as supported by previous studies using IR spectroscopy, XPS, quartz crystal microbalance, and elemental analysis conducted by Maksymiuk[3]. The blue shift can be associated with a decrease in conductivity because it indicates a widening of the band gap energy. As the conjugation length decreases and doping anions are released, the electronic structure of the polymer is altered, increasing the band gap[30],[31].

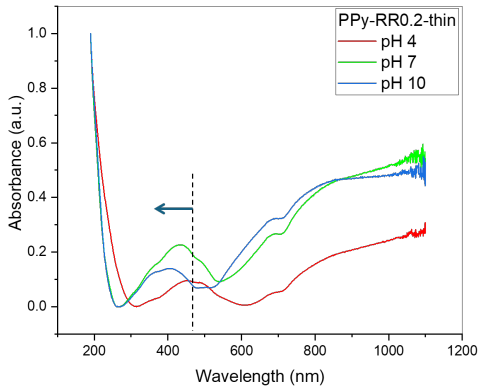

(a) Normalized UV-vis spectrum of thin PPy with RR 0.2 at pH 4, 7, and 10

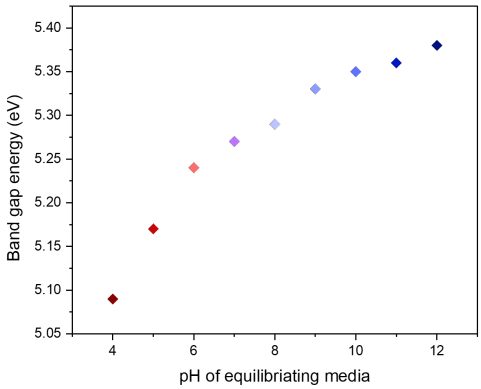

(b) Band gap change of PPy with RR 0.2 at different pH levels

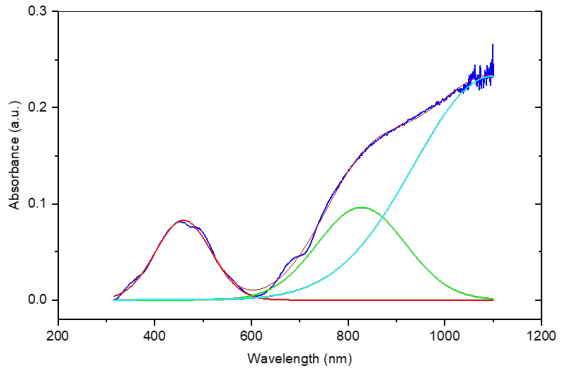

(c) Deconvoluted UV-vis spectra of PPy 0.2 thin at pH 4

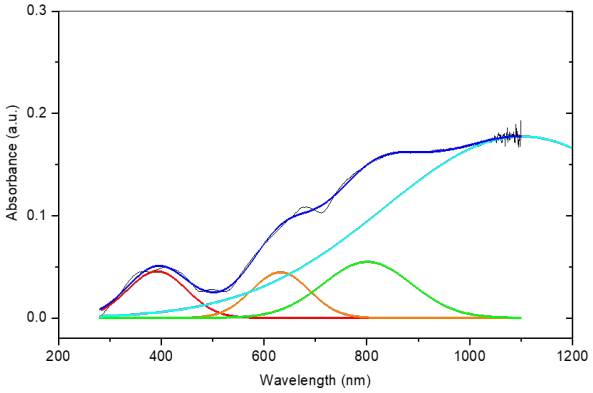

(d) Deconvoluted UV-vis spectra of PPy 0.2 thin at pH 10

Figure 4: Effect of pH on oCVD PPy films

4.1.1 Thickness

Several film parameters are suspected to influence the optical band gap of PPy because the parameters can significantly alter the materials electronic structure, crystallinity, and morphology[2],[5]. The first parameter that was investigated was the deposition time and thus the thickness of the PPy films. Thickness plays a significant role in this context because, in oCVD, polymerization and doping occur simultaneously. As a result, thicker films are expected to have a higher initial doping concentration due to the greater amount of material available. In Figure 5 the optical band gap of thin (+/-100nm) and thick (+/-300nm) samples were measured at pH 4, 7 and 10. The Tauc plots originating from the UV-vis measurements are depicted in Figure 14. The thin oCVD PPy film has a band gap of 5.09 eV at pH 4 which increases upon equilibriation in higher pH. The thick film has an initial band gap of 4.92 and increases to 5.26 at higher pH (pH 10). In both thin and thick films, an increase in band gap was seen with increasing pH. This increase was explained in the previous section (subsubsection 4.1.2). In addition, it can be seen that the thick oCVD PPy films possess a lower optical band gap compared to the thin samples.

A thick surface is expected to have fewer imperfections that scatter and resist the movement of conducting electrons. This effect results in a lower band gap. In thinner samples, the imperfections of the substrate are directly translated into the polymer layer. The movement of charge is limited by scattering against these imperfections. In thicker samples, the imperfections are flattened out by the polymer layer because more material is provided[3]. Han Wu et al. saw a similar effect; generally, they saw the conductivity would rise with the increase of coating thickness and then it would be saturated. However, they saw that a further thickness increase of the coating would limit the electron supply through a thick insulating layer, leading to a decreased conductivity.[32]. Maksymiuk supports the limitations of electron transport within thick films[3]. More variations of thickness have to be evaluated to confirm if this effect also affects the band gap.

Moreover, a thicker surface is expected to have a higher doping concentration compared to thinner samples because it can incorporate more dopant ions throughout its greater volume. For the same equilibration time, the counter-ion exchange in thick films is lower compared to thin films due to diffusion limitations in the thicker films[3],[11]. In thicker films, the increased material thickness presents a barrier to the efficient movement of counter ions, slowing the exchange process. Consequently, there is a smaller change in the band gap of thicker films compared to thinner films. Kaufman et al.[11] demonstrated that the polaron-bipolaron transition is a kinetic phenomenon limited by the rate of counter-ion diffusion. In thinner films, the shorter distance for ion movement allows for more efficient and rapid counter-ion exchange, resulting in more significant changes in band gap. Since thinner films exhibit a larger change in band gap compared to thicker films, it indicates that thinner oCVD PPy films are more sensitive to pH changes. The greater responsiveness of thinner films to environmental conditions makes them more suitable for applications such as pH sensors, where detecting small changes is crucial. Therefore, despite their higher band gap, thin films have been chosen for further investigation for use in pH sensors.

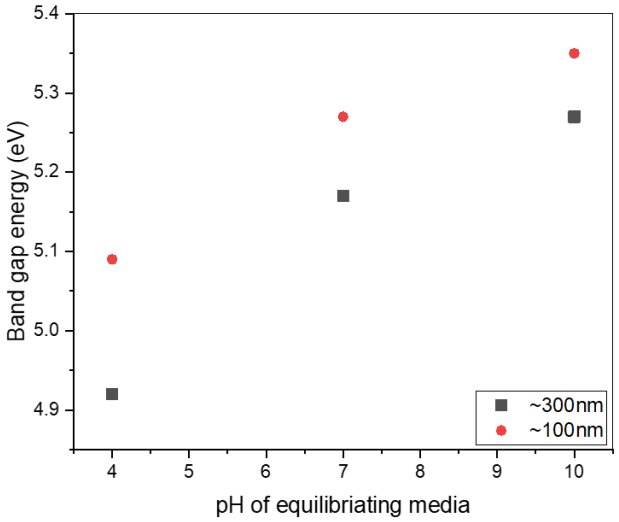

Figure 5: Optical band gap of thin and thick PPy samples plotted against the pH of the equilibriating media

4.1.2 Reaction Ratio

Another parameter investigated is the stoichiometric ratio of oxidant to monomer (reaction ratio). In Figure 6 RR of 0.1-0.3 is plotted against the pH of the equilibriating media. The Tauc plots originating from the UV-vis measurements are depicted in Figure 15. It is seen that a reaction ratio of 0.2 results in the lowest band gap of 5.09 and 5.27 eV at pH 4 and 7 respectively. A big increase in band gap is observed with increasing pH (5.35 eV at pH 10), indicating a high pH sensitivity. Furthermore, it can be observed that an RR of 0.3 has the highest band gap of the three evaluated RR of 5.29 and 5.33 eV at pH 4 and 7 respectively. Moreover, this RR showed the least increase of band gap with increasing pH. Moreover, a reaction ratio of 0.1 showed an intermediate band gap compared to 0.2 and 0.3 with a band gap of 5.17 and 5.31 at pH 4 and 7 respectively. At pH 10 the different reaction ratios result in similar band gaps (5.35 eV).

The reaction ratio affects the band gap as the oxidant concentration directly affects the doping concentration. The chlorine from the antimony pentachloride oxidant acts as the dopant and the oxidant. Therefore, finding the optimal oxidant concentration is crucial for ensuring high conductivity. Doping stabilizes the charge of the polarons and bipolarons within the material. It is suspected that a reaction ratio of 0.1 exhibits a higher optical band gap compared to a ratio of 0.2 due to underdoping. Underdoping means that fewer charge carriers are introduced into the material during the doping process. Lower doping levels, as seen with the 0.1 reaction ratio, result in fewer polaron states being introduced, which in turn leads to a higher optical band gap. The conductivity data from Dianatdar et al. corroborates this trend observed with reaction ratios from 0.1 to 0.2. Their findings support the influence of doping levels on the optical band gap, confirming the impact of the reaction ratio on the material's electronic properties[2].

Furthermore, the band gap of RR 0.3 is suspected to be the highest because of overoxidation caused by the higher oxidant concentration. Dianatdar et al.[2] support the overoxidation as a result of a higher reaction ratio. They evaluated XPS data to find the doping level and relate it with conductivity. The number of Cl^- counter ions

per pyrrole ring indicates the doping level, which can be measured using the Cl/N ratio obtained by XPS. The optimal doping level was found to be two counter ions for every three pyrrole rings (N/Cl = 1.4). However, increasing the oxidant concentration reduced the N/Cl ratio in the resulting film to approximately 0.35. This implies an average of three Cl^- ions per pyrrole ring, indicating overdoping or overoxidation[2]. This overpopulation of negative charges (chlorine ions) restricts the conductivity of electrons. In addition, their XPS data shows increased carbon content due to defects such as ring cleavage, PPy chain cross-linking and aliphatic chain formation. The defects could result in lower conjugation length and lower polaron/bipolar concentration with as a result a higher optical band gap[2],[33].

At pH 10, all three reaction ratios showed similar optical band gap energies. This observation can be attributed to the deprotonation of the charged structures at this higher pH level. Deprotonation results in a higher concentration of the neutral complex and a lower concentration of polarons and bipolarons. In this deprotonated state, the material primarily consists of neutral polypyrrole, which is not affected by the doping concentration because it lacks any charge. Therefore, regardless of the doping levels and corresponding reaction ratios, the resulting optical band gap is unaffected[3].

For the application of PPy as a pH sensor, sensitivity to pH is a crucial factor. As shown in Figure 6, a reaction ratio of 0.2 not only results in the lowest optical band gap energy but also exhibits the steepest increase, indicating the highest pH sensitivity. The significant difference in optical band gap facilitates easier detection. For this reason, the PPy thin film with a reaction ratio of 0.2 was found to be the most optimal.

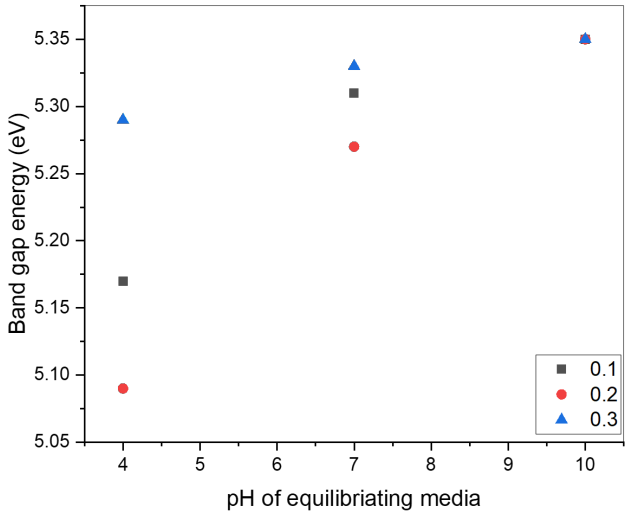

Figure 6: Band gap energy change with pH, comparison of reaction ratios

4.1.3 Long-term effects

Thereafter, the long-term effects of pH solutions on the PPy film were investigated. In Figure 7 the short- and long-term band gap energies are plotted against the pH of the equilibriating media. The Tauc plots originating from the UV-vis measurements are depicted in Figure 17. A similar trend is observed when comparing the short- and long-term data. At pH 4 the long-term samples exhibit a higher gap. However, with increasing pH the band gap of the long-term samples is lower than the short-term band gaps. The highest difference in band gap measured was 0.06 eV. A decrease in band gap energy measured by UV-vis spectroscopy can arise from changes in material properties. Swelling, for instance, is a phenomenon that can alter the Tauc plot, subsequently affecting the calculated band gap energy. Swelling occurs when a material absorbs solvent molecules or undergoes structural changes, leading to an expansion in volume. Consequently, when the material is swollen, the Tauc plot may exhibit shifts or distortions.[12],[20],[34].

Investigation into the polaron bipolaron band transition in PPy by Scott et al.[11] suggests that the recombination of polarons to the more conductive bipolarons is the reason for the lower band gap. It is stated that the rearrangement is a slow process controlled by ionic mass transport. Therefore, it is believed that counter-ion diffusion is the kinetically limiting step in polaron recombination and that the thermodynamic equilibrium is not

achieved during the observation time of several hours. Thus, after longer submersion, a situation closer to equilibrium is seen that results in a lower band gap and in turn a higher conductivity. This explanation corresponds well to the observed trend. However, swelling could still play a minor role in long-term measurements[3],[11],[34].

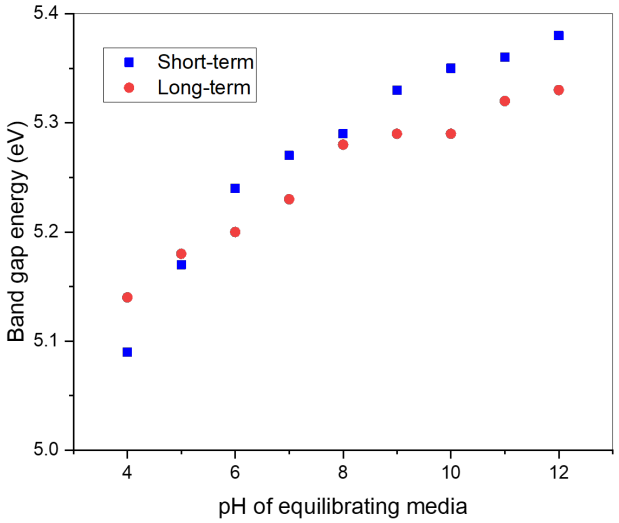

Figure 7: Long-term effect of pH on the band gap energy

4.2 Effect of electrolytes on the performance of oCVD PPy

4.2.1 Profilometry

In the following section, the properties of PPy in its application as a supercapacitor material are investigated. Various thicknesses are evaluated using different electrolytes. The thickness is adjusted by varying the nitrogen patch flow and the position in the reactor, as described in the methods section. To measure the exact thickness of the prepared samples, profilometry was used. The results of the profilometry measurements are depicted in Figure 8. It can be observed that initially, increasing the nitrogen patch flow causes a decrease in thickness, followed by an increase (Row 2). In Row 3, only an increase in thickness is observed.

This behaviour can be explained by a dual role of nitrogen in the oCVD process. At lower flow rates, nitrogen is suspected to act as a diluent, reducing the concentration of reactive species and thus decreasing the polymerization rate, which results in thinner films. As the flow rate increases, nitrogen is expected to transition to acting as a carrier gas, improving the transport and mixing of reactive species at the substrate surface. This enhances the polymerization rate, leading to thicker films. Thus, nitrogen initially decreases the thickness by dilution at lower flow rates and subsequently increases it by acting as a carrier gas at higher flow rates. For Row 3 the nitrogen is expected to only increase transports of the reactive species throughout the chamber, ensuring a higher concentration of monomer and oxidant at the substrate surface[2],[5].

The influence of nitrogen patch flow on the properties of oCVD PPy has not been studied until now. Yuan et al.[35] explored the impact of nitrogen patch flow on a different compound, discovering that it enhances both the doping concentration and uniformity of the resulting films. In Figure 8, it is observed that row 3 has a lower standard deviation compared to row 2. This depicts that row 3 has higher uniformity compared to row 2. Furthermore, observations and profilometer measurements revealed that the samples of row 2 exhibited regions of varying thickness, indicating significant inhomogenity across the surface. Further research has to be done on the effect of nitrogen flow on the thickness, uniformity and doping levels.

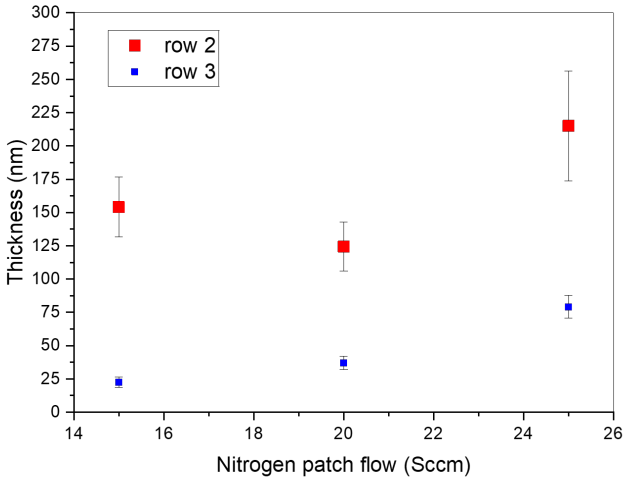

Figure 8: Profilometry measurements for increasing nitrogen patch flow and changing reactor position

4.2.2 Contact Angle

Next, the contact angle was measured, since achieving high wettability (low contact angle) is essential for facilitating efficient ion transport between the electrolyte and the electrode surface in a supercapacitor[10]. The contact angle measurements of the different electrolytes are plotted against the thickness in Figure 9. Images of the contact angle measurements are depicted in Figure 10. No significant change in contact angle is observed with increasing thickness according to the t-test. A contradictory effect was seen by Koduru et al. They observed an increase in the contact angle with increasing thickness, attributed to a smoother surface with fewer defects[8]. The thickness of the samples used in this thesis was varied using the nitrogen patch flow. This parameter appears to produce different effects compared to changing the deposition time.

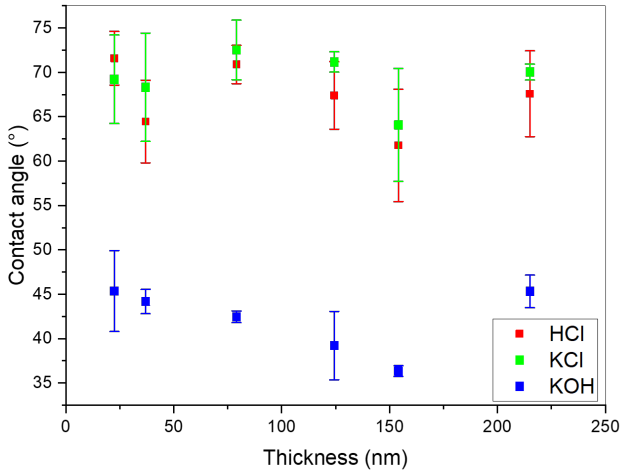

Figure 9: Contact angle measurements using KCl, HCl and KOH droplets

Furthermore, the t-test indicates that there is no significant difference in the contact angles between KCl and HCl. This result can be caused by the inaccuracy of the contact angle measurement. High standard deviations are observed, mainly caused by the time dependence of the contact angle measurement[8]. Moreover, the previously mentioned inhomogeneity of the samples could have caused the high standard deviation and inaccuracy of the measurements. To investigate the wetting of PPy using different electrolyte solutions, timed measurements should be taken at multiple times[8]. This method is called the dynamic contact angle. Dynamic contact angle measurements can help assess how effectively the electrolyte solution wets and penetrates the PPy film over time, which is crucial for efficient charge transport and ion diffusion within the material[8],[23],[25]. Koduru et al.[8] showed that with time the contact angle decreases significantly. The measurements done in this thesis could be inaccurate due

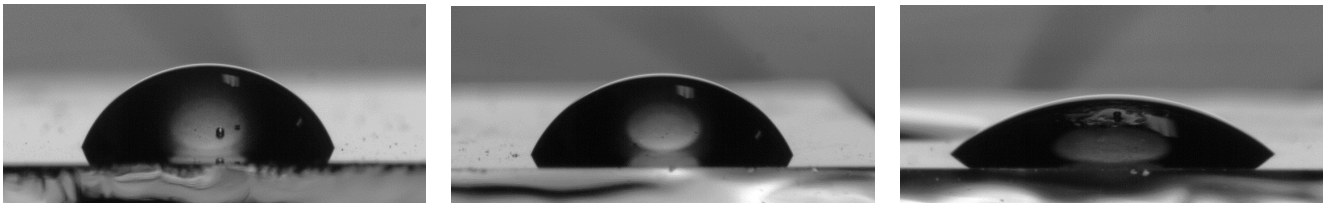

(a) Contact angle KCl on 215nm film (b) Contact angle HCl on 215nm film (c) Contact angle KOH on 215nm film

Figure 10: Contact angle of 215nm film of three electrolyte solutions

to being measured at slightly different times. Further research has to be done to investigate the effect of film thickness on the contact angle by doing dynamic contact angle measurements.

In addition, from Figure 9 a significant decrease in contact angle is observed when depositing KOH droplets on the PPy film. It is suspected that this decrease in contact angle is caused by an increase in surface roughness caused by delamination. When considering wetting, behaviour on solid surfaces is governed by several models. Wenzel model describes the wetting behaviour of a rough surface, where the liquid fills the cavities induced by surface roughness. In contrast, in the Cassie-Baxter model, the cavities are filled by air bubbles. In the case of PPy, its wetting behaviour would align more closely with the Wenzel model. The surface roughness of PPy and the lack of significant air pockets suggest that its wetting behaviour aligns more closely with the Wenzel model rather than the Cassie-Baxter model. This is supported by literature[25]. According to the Wenzel model, increased surface roughness enhances the interaction and surface area between the solvent and the film, resulting in a decreased contact angle. Mahmoodian et al. support the theory of surface roughness with the use of SEM and AFM. Additionally, they saw a direct relationship between surface roughness and contact angle[25],[36]. Another theory by Wernet and Wegner suggests that treatment of polypyrrole with OH^- ions results in the chemical incorporation of this ion onto the polymer backbone, thus disrupting the conjugation and the morphology of the film[30]. The incorporation of OH^- ions is suspected to cause the delamination and increase of surface roughness that is observed. Pictures of the PPy surface after contact with KCl/HCL and KOH are depicted in Figure 11 and Figure 12 respectively. In these pictures, clear imperfections and cracks are observed on the surface that is treated with KOH. In contrast, the surface treated with HCL/KCL showed almost no defects.

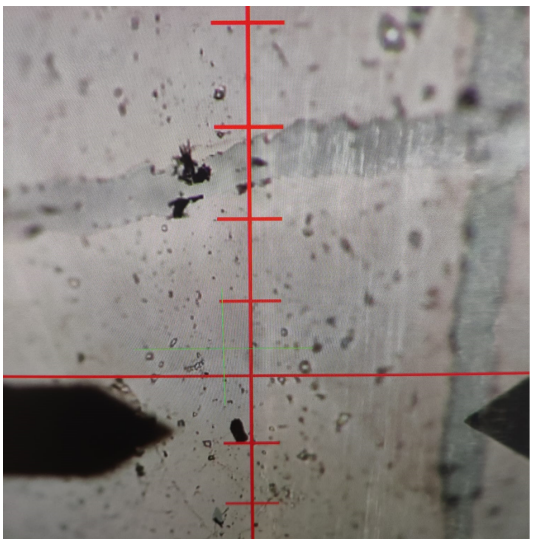

Figure 11: Surface of oCVD PPy after KCl and HCl treatment

4.2.3 Four-point probe

Four-point probe measurement was done to further investigate the effect of thickness and electrolyte solutions on the conductivity. The measurements are depicted in Figure 13. In the pristine samples (Figure 13a) a decrease in conductivity with increasing thickness is observed. The increase observed between 124nm and 154nm is considered insignificant based on the results of a t-test and the high standard deviation. The decreasing conductivity trend is contradictory to the decrease in the optical band gap that was observed previously. It turns out that thickness

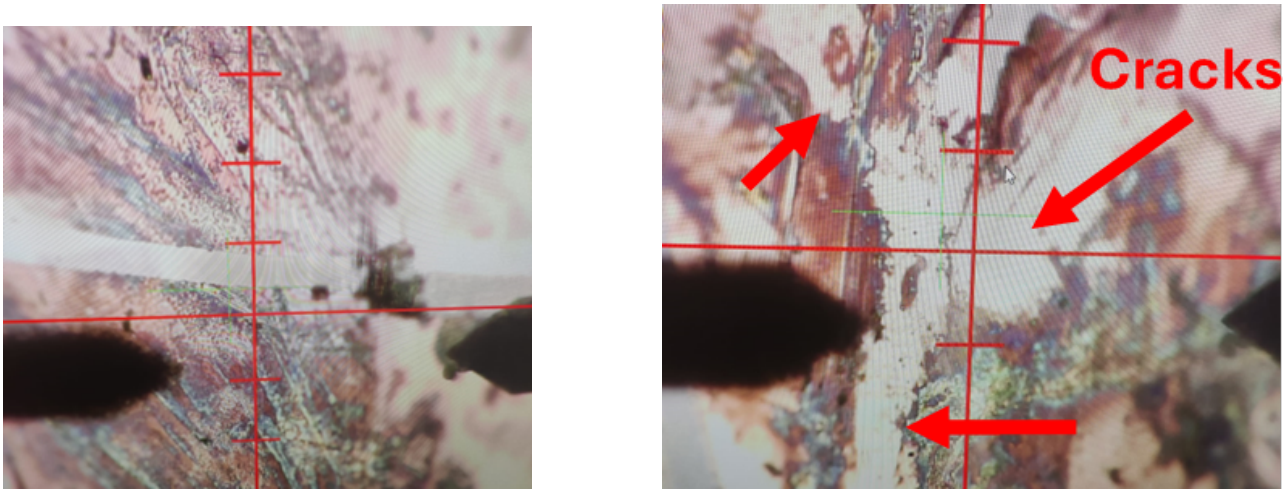

(a) Surface of oCVD PPy after KOH treatment

(b) Cracks in oCVD PPy surface depicted by arrows

Figure 12: Observed cracks on oCVD PPy surface

change due to nitrogen patch flow differs from the one due to deposition time. One explanation for the decrease in conductivity can be related to the doping concentration. Due to changing the nitrogen patch flow the oxidant concentration increases as the nitrogen facilitates higher transport rates. The increase in oxidant concentration causes overoxidation as seen previously when varying the reaction ratio (subsubsection 4.1.2). Therefore, with increasing nitrogen patch flow the conductivity decreases as a result of overoxidation[2],[3].

In Figure 13b and Figure 13c, the conductivity measurements of KCl and HCl are presented, respectively. Both KCl and HCl are salts that introduce Cl^- ions into the solution. In row 3 a decrease in conductivity is seen for KCl and HCl. This can be attributed to the introduction of additional doping ions, which in turn causes overoxidation[3]. This results in the lowered conductivity that was observed. In row 2, slight overoxidation is seen as mentioned previously. The introduction of the KCl and HCl then causes dedoping as the salts can accept the Cl^- ions. As a result, the doping concentration decreases and the conductivity increases[2],[33]. The reason and significance of the observed outliers in the data have to be investigated further.

In Figure 13d the conductivity measurements of KOH is depicted. Negligible conductivity was detected. The decrease in conductivity compared to KCl and HCl is suggested to be caused by the observed delamination and increased surface roughness and imperfections caused by KOH. The previously mentioned theory by Wernet and Wegner states that treatment of polypyrrole with OH^- ions results in the chemical incorporation of this ion onto the polymer backbone, thus disrupting the conjugation and the morphology of the film[30]. The incorporation of OH^- ions is suspected to cause the decrease in conductivity. Thus, due to the cracks, imperfections and the incorporation of the OH^- ions, the contact resistance of the four-point probe is expected to be of such high value that no conductivity remains[23],[24],[26]. In addition, long-term samples submerged in KOH showed complete delamination from the substrate. This further underscores the unsuitability of KOH as a supercapacitor material.

However, the four-point probe method measures the sheet resistance of a material, which is highly surface-sensitive. This can be problematic if the surface properties of the thin film differ significantly from its bulk properties. Additionally, while the technique is designed to minimize contact resistance, any surface contamination or oxidation can still affect the measurement accuracy. Moreover, cracks in the surface can significantly alter the results. The method also assumes uniform thickness and conductivity across the film, so any variations can lead to inaccurate results. As determined by the profilometry, the samples that were used were highly inhomogeneous. Moreover, the measuring depth of the four-point probe is limited to the near-surface region, which may not be representative of the entire film bulk properties[26]. Due to all these reasons, differences between the UV-vis measurement and four-point probe are likely to be seen. The UV-Vis measurements are expected to yield more reliable results, as the four-point probe method is limited to surface properties. UV-vis measurements could be done for electrolyte solutions to obtain the band gap and the bulk properties. The limits of the four-point probe should be kept in mind.

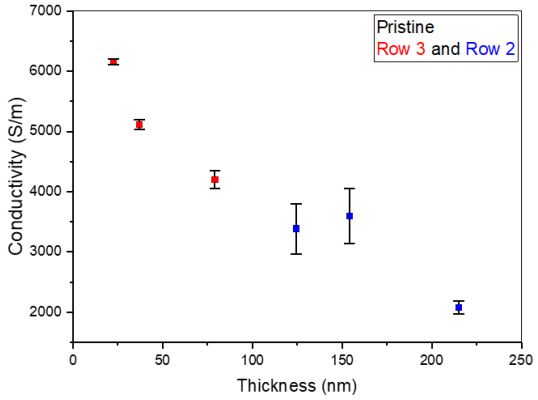

(a) Conductivity of pristine sample

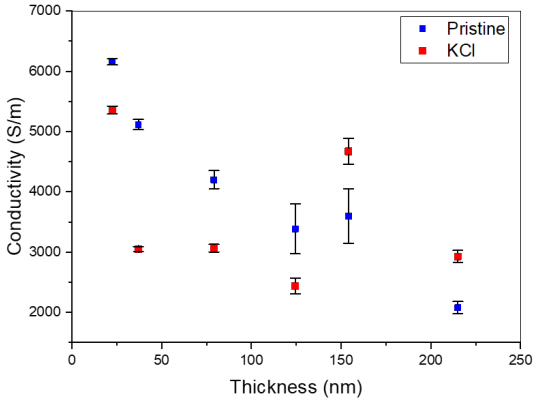

(b) Conductivity of KCl treated samples

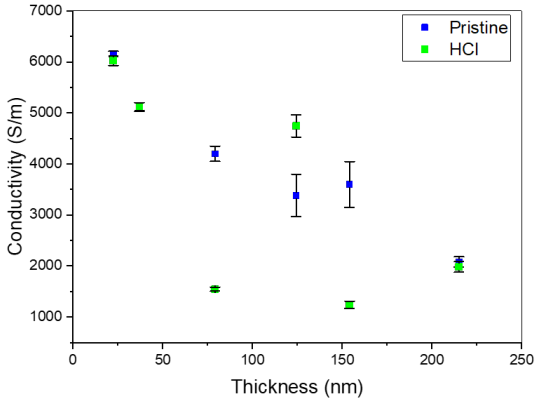

(c) Conductivity of HCl treated samples

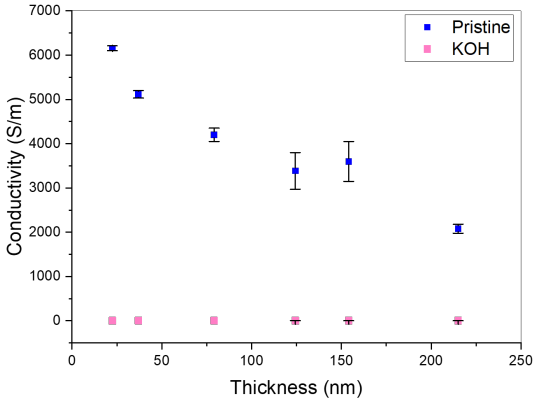

(d) Conductivity of KOH treated samples

Figure 13: Conductivity calculated using four-point probe, using different electrolyte solutions

5 Future Perspectives

One crucial area for future exploration is delving into the mechanisms behind the observed delamination and surface roughness induced by KOH. In addition, exploring more alternative electrolyte compositions could offer insights into enhancing the performance of PPy-based devices. Furthermore, the effect of nitrogen patch flow on the PPy film has not yet been extensively investigated. Therefore, it could be an interesting parameter for additional research. Lastly, while this study demonstrated the long-term stability of PPy films, further research is necessary to investigate potential changes in material properties over more extended periods than five days. Examining the effects of prolonged exposure to different pH solutions and electrolytes on swelling behaviour, and performance could provide valuable insights into the durability and reliability of PPy films for practical applications.

6 Conclusion

This study investigated the effects of environmental conditions on the performance of oCVD polypyrrole thin films. The effect of pH on the band gap and the performance of PPy when using different electrolyte solutions was highlighted, as the focus lay on the application as a pH sensor and as a supercapacitor material. Firstly, regarding the influence of pH, it was observed that the optical band gap of PPy thin films increases with pH. This phenomenon was attributed to the deprotonation of polarons and bipolarons, resulting in a higher concentration of neutral PPy structures. This was supported by deconvolution of the UV-vis data. Moreover, a blue shift in the UV-vis spectra with increasing pH levels was noted, indicating a decrease in conjugation length and the release of doping anions, ultimately leading to a wider band gap. Additionally, it was found that thicker films exhibit lower optical band gaps due to having fewer surface imperfections. The conductive electrons are resisted by these imperfections causing lower conductivity and higher band gap for thinner samples. In thicker samples, the imperfections are flattened by the provided material. Furthermore, a reaction ratio of 0.2 was found to be the most

favourable to avoid underdoping or overoxidation. Moreover, the reaction ratio of 0.2 showed the highest sensitivity to pH, facilitating accurate and easy measuring. These findings suggest that pH, thickness and reaction ratio play a crucial role in modulating the electronic and optical properties of PPy, which is essential for various applications. For pH sensors, the ideal case in this thesis was found to be a thin film ($\tilde{1}$00nm) with a reaction ratio of 0.2.

Secondly, to investigate the performance of PPy as a supercapacitor material, not only the electrolyte solutions was changed, but also the nitrogen patch flow and the reactor position. Profilometry depicted that an increasing nitrogen patch flow initially acts as a diluent and then acts as a carrying agent. In addition, more uniformity was observed in row 3 compared to row 2. Furthermore, it was observed that electrolyte treatments significantly influenced the contact angle and conductivity of the films when using KOH. Contact angle measurements demonstrated that electrolyte treatments influenced wetting properties, with KCl and HCl treatments showing similar behaviour, while KOH treatment resulted in decreased contact angles attributed to increased surface roughness and cracks caused by delamination. Four-point probe conductivity measurements revealed varying trends among electrolyte-treated samples, with KCl and HCl-treated samples exhibiting lower conductivity in row 3, possibly due to the introduction of Cl^- ions causing overoxidation. Furthermore, in row 2 an increase in conductivity was observed. This was attributed to the dedoping of the overoxidized samples. KOH-treated samples showed negligible conductivity, likely due to surface imperfections, delamination and cracks in the surface. This research showed that KOH is not a suitable electrolyte for PPy.

Lastly, the long-term stability of PPy thin films was examined. Long-term stability studies indicated decreased band gap measurements over time. It was suggested that the rearrangement of polarons to bipolarons was a slow process that came closer to equilibrium at longer submersion times. Thus, causing a higher bipolaron concentration and a lower band gap. However, it was acknowledged that swelling effects from prolonged exposure to solutions could potentially influence band gap measurements.

In summary, this study provides valuable insights into the factors influencing the properties of PPy thin films and their potential applications. Moreover, the importance of considering environmental impact, such as pH and electrolyte effects, was emphasized. Further research is required to elucidate the underlying mechanisms behind the observed effects and to address the limitations of the experimental methods employed.

7 Acknowledgements

I would like to extend my heartfelt appreciation to my daily supervisors, Adrivit Mukherjee and Fika Fauzi, for their consistent support in the laboratory and throughout the entire process. Their guidance, collaboration and assistance have been very helpful. I am also grateful to Professor Ranjita Bose for her invaluable weekly meetings, where her expertise and feedback significantly contributed to refining my work.

8 References

[1] R. Ansari, "Polypyrrole Conducting Electroactive Polymers: Synthesis and Stability Studies," *E-Journal of Chemistry*, vol. 3, no. 4, pp. 186–201, 2006, ISSN: 0973-4945. DOI: 10.1155/2006/860413.

[2] A. Dianatdar, M. Miola, O. De Luca, P. Rudolf, F. Picchioni, and R. K. Bose, "All-dry, one-step synthesis, doping and film formation of conductive polypyrrole," *Journal of Materials Chemistry C*, vol. 10, no. 2, pp. 557–570, 2022, ISSN: 2050-7526. DOI: 10.1039/D1TC05082F.

[3] K. Maksymiuk, "Chemical Reactivity of Polypyrrole and Its Relevance to Polypyrrole Based Electrochemical Sensors," *Electroanalysis*, vol. 18, no. 16, pp. 1537–1551, Aug. 2006, ISSN: 1040-0397. DOI: 10.1002/elan.200603573.

[4] M. Trojanowicz, "Application of Conducting Polymers in Chemical Analysis," *Microchimica Acta*, vol. 143, no. 2-3, pp. 75–91, Dec. 2003, ISSN: 0026-3672. DOI: 10.1007/s00604-003-0066-5.

[5] W. E. Tenhaeff and K. K. Gleason, "Initiated and Oxidative Chemical Vapor Deposition of Polymeric Thin Films: iCVD and oCVD," *Advanced Functional Materials*, vol. 18, no. 7, pp. 979–992, Apr. 2008, ISSN: 1616-301X. DOI: 10.1002/adfm.200701479.

[6] A. Mukherjee, A. Dianatdar, M. Z. Gładysz, *et al.*, "Electrically Conductive and Highly Stretchable Piezoresistive Polymer Nanocomposites via Oxidative Chemical Vapor Deposition," *ACS Applied Materials & Interfaces*, vol. 15, no. 26, pp. 31 899–31 916, Jul. 2023, ISSN: 1944-8244. DOI: 10.1021/acsami.3c06015.

[7] A. Dianatdar and R. K. Bose, "Oxidative chemical vapor deposition for synthesis and processing of conjugated polymers: a critical review," *Journal of Materials Chemistry C*, vol. 11, no. 35, pp. 11 776–11 802, 2023, ISSN: 2050-7526. DOI: 10.1039/D3TC01614E.

[8] H. K. Koduru, L. Marino, J. Vallivedu, C.-J. Choi, and N. Scaramuzza, "Microstructural, wetting, and dielectric properties of plasma polymerized polypyrrole thin films," *Journal of Applied Polymer Science*, vol. 133, no. 38, Oct. 2016, ISSN: 0021-8995. DOI: 10.1002/app.43982.

[9] F. Yue, T. S. Ngin, and G. Hailin, "A novel paper pH sensor based on polypyrrole," *Sensors and Actuators B: Chemical*, vol. 32, no. 1, pp. 33–39, Apr. 1996, ISSN: 09254005. DOI: 10.1016/0925-4005(96)80106-7.

[10] A. Yavuz, N. Ozdemir, and H. Zengin, "Polypyrrole-coated tape electrode for flexible supercapacitor applications," *International Journal of Hydrogen Energy*, vol. 45, no. 38, pp. 18 876–18 887, Jul. 2020, ISSN: 03603199. DOI: 10.1016/j.ijhydene.2020.05.124.

[11] J. H. Kaufman, N. Colaneri, J. C. Scott, and G. B. Street, "Evolution of Polaron States into Bipolarons in Polypyrrole," *Physical Review Letters*, vol. 53, no. 10, pp. 1005–1008, Sep. 1984, ISSN: 0031-9007. DOI: 10.1103/PhysRevLett.53.1005.

[12] J. Edberg, D. Iandolo, R. Brooke, *et al.*, "Patterning and Conductivity Modulation of Conductive Polymers by UV Light Exposure," *Advanced Functional Materials*, vol. 26, no. 38, pp. 6950–6960, Oct. 2016, ISSN: 1616-301X. DOI: 10.1002/adfm.201601794.

[13] M. M. Abdi, H. N. M. Ekramul Mahmud, L. C. Abdullah, A. Kassim, M. Zaki Ab. Rahman, and J. L. Y. Chyi, "Optical band gap and conductivity measurements of polypyrrole-chitosan composite thin films," *Chinese Journal of Polymer Science*, vol. 30, no. 1, pp. 93–100, Jan. 2012, ISSN: 0256-7679. DOI: 10.1007/s10118-012-1093-7.

[14] M. M. Abdi, H. N. M. Ekramul Mahmud, L. C. Abdullah, A. Kassim, M. Zaki Ab. Rahman, and J. L. Y. Chyi, "Optical band gap and conductivity measurements of polypyrrole-chitosan composite thin films," *Chinese Journal of Polymer Science*, vol. 30, no. 1, pp. 93–100, Jan. 2012, ISSN: 0256-7679. DOI: 10.1007/s10118-012-1093-7.

[15] F. Yue, T. S. Ngin, and G. Hailin, "A novel paper pH sensor based on polypyrrole," *Sensors and Actuators B: Chemical*, vol. 32, no. 1, pp. 33–39, Apr. 1996, ISSN: 09254005. DOI: 10.1016/0925-4005(96)80106-7.

[16] M. Qin, H. Guo, Z. Dai, X. Yan, and X. Ning, "Advances in flexible and wearable pH sensors for wound healing monitoring," *Journal of Semiconductors*, vol. 40, no. 11, p. 111 607, Nov. 2019, ISSN: 1674-4926. DOI: 10.1088/1674-4926/40/11/111607.

[17] A. M. Saleem, V. Desmaris, and P. Enoksson, "Performance Enhancement of Carbon Nanomaterials for Supercapacitors," *Journal of Nanomaterials*, vol. 2016, pp. 1–17, 2016, ISSN: 1687-4110. DOI: 10.1155/2016/1537269.

[18] Mart Hendriksen, "mCEng_2021_HendriksenM.pdf," *RUG*, 2021.

[19] P. Rapta, A. Petr, and L. Dunsch, "Conducting polymers at electrode surfaces as studied by in situ ESR/UV-Vis-NIR spectroscopy," *Synthetic Metals*, vol. 119, no. 1-3, pp. 409–410, Mar. 2001, ISSN: 03796779. DOI: 10.1016/S0379-6779(00)01164-4.

[20] P. Makuła, M. Pacia, and W. Macyk, "How To Correctly Determine the Band Gap Energy of Modified Semiconductor Photocatalysts Based on UV–Vis Spectra," *The Journal of Physical Chemistry Letters*, vol. 9, no. 23, pp. 6814–6817, Dec. 2018, ISSN: 1948-7185. DOI: 10.1021/acs.jpclett.8b02892.

[21] J. Klein, L. Kampermann, B. Mockenhaupt, M. Behrens, J. Strunk, and G. Bacher, "Limitations of the Tauc Plot Method," *Advanced Functional Materials*, vol. 33, no. 47, Nov. 2023, ISSN: 1616-301X. DOI: 10.1002/adfm.202304523.

[22] B. J. Mrstik, P. J. McMarr, J. R. Blanco, and J. M. Bennett, "Measurement of the Thickness and Optical Properties of Thermal Oxides of Si Using Spectroscopic Ellipsometry and Stylus Profilometry," *Journal of The Electrochemical Society*, vol. 138, no. 6, pp. 1770–1778, Jun. 1991, ISSN: 0013-4651. DOI: 10.1149/1.2085871.

[23] J. V. Thombare, G. M. Lohar, S. K. Shinde, S. S. Dhasade, M. C. Rath, and V. J. Fulari, "Synthesis, characterization and surface wettability study of polypyrrole films: Effect of applied constant current density," *Electronic Materials Letters*, vol. 11, no. 2, pp. 266–270, Mar. 2015, ISSN: 1738-8090. DOI: 10.1007/s13391-014-4082-x.

[24] Z. Huang, C. Pan, P. Huang, *et al.*, "Effects of ZnO nanoparticles on the microstructure, mechanical properties and wettability of polypyrrole–polydopamine nanocomposites coated on W substrate," *Materials Today Communications*, vol. 28, p. 102 620, Sep. 2021, ISSN: 23524928. DOI: 10.1016/j.mtcomm.2021.102620.

[25] J. H. Chang, "Tunable Wettability of Microstructured Polypyrrole Films," Tech. Rep., 2008.

[26] I. Miccoli, F. Edler, H. Pfnür, and C. Tegenkamp, "The 100th anniversary of the four-point probe technique: the role of probe geometries in isotropic and anisotropic systems," *Journal of Physics: Condensed Matter*, vol. 27, no. 22, p. 223 201, Jun. 2015, ISSN: 0953-8984. DOI: 10.1088/0953-8984/27/22/223201.

[27] K. Yakushi, L. J. Lauchlan, T. C. Clarke, and G. B. Street, "Optical study of polypyrrole perchlorate," *The Journal of Chemical Physics*, vol. 79, no. 10, pp. 4774–4778, Nov. 1983, ISSN: 0021-9606. DOI: 10.1063/1.445621.

[28] F. Tavoli and N. Alizadeh, "In situ UV–vis spectroelectrochemical study of dye doped nanostructure polypyrrole as electrochromic film," *Journal of Electroanalytical Chemistry*, vol. 720-721, pp. 128–133, Apr. 2014, ISSN: 15726657. DOI: 10.1016/j.jelechem.2014.03.022.

[29] J. C. Scott, P. Pfluger, M. T. Krounbi, and G. B. Street, "Electron-spin-resonance studies of pyrrole polymers: Evidence for bipolarons," *Physical Review B*, vol. 28, no. 4, pp. 2140–2145, Aug. 1983, ISSN: 0163-1829. DOI: 10.1103/PhysRevB.28.2140.

[30] M. Forsyth and V.-T. Truong, "A study of acid/base treatments of polypyrrole films using 13C n.m.r. spectroscopy," *Polymer*, vol. 36, no. 4, pp. 725–730, Jan. 1995, ISSN: 00323861. DOI: 10.1016/0032-3861(95)93101-Q.

[31] R. H. Baughman and L. W. Shacklette, "Conductivity as a function of conjugation length: Theory and experiment for conducting polymer complexes," *Physical Review B*, vol. 39, no. 9, pp. 5872–5886, Mar. 1989, ISSN: 0163-1829. DOI: 10.1103/PhysRevB.39.5872.

[32] H. Wu, S. Shen, J. Li, X. Chen, Z. Zhang, and W. Ou-Yang, "Boosted field emission properties and thickness effect of conductive polymers coated silicon carbide matrices for vacuum electronic devices," *Vacuum*, vol. 180, p. 109 594, Oct. 2020, ISSN: 0042207X. DOI: 10.1016/j.vacuum.2020.109594.

[33] L. Atanasoska, K. Naoi, and W. H. Smyrl, "XPS studies on conducting polymers: polypyrrole films doped with perchlorate and polymeric anions," *Chemistry of Materials*, vol. 4, no. 5, pp. 988–994, Sep. 1992, ISSN: 0897-4756. DOI: 10.1021/cm00023a012.

[34] K. Xie, A. Glasser, S. Shinde, *et al.*, "Delamination and Wrinkling of Flexible Conductive Polymer Thin Films," *Advanced Functional Materials*, vol. 31, no. 21, May 2021, ISSN: 1616-301X. DOI: 10.1002/adfm.202009039.

[35] W. Yuan, Y. Pei, N. Guo, Y. Li, X. Zhang, and X. Liu, "The Optimizing Effect of Nitrogen Flow Ratio on the Homoepitaxial Growth of 4H-SiC Layers," *Crystals*, vol. 13, no. 6, p. 935, Jun. 2023, ISSN: 2073-4352. DOI: 10.3390/cryst13060935.

[36] M. Mahmoodian, B. Pourabbas, and S. Mohajerzadeh, "Effect of anionic dopants on thickness, morphology and electrical properties of polypyrrole ultra-thin films prepared by in situ chemical polymerization," *Thin Solid Films*, vol. 583, pp. 255–263, May 2015, ISSN: 00406090. DOI: 10.1016/j.tsf.2015.03.043.

9 Appendices

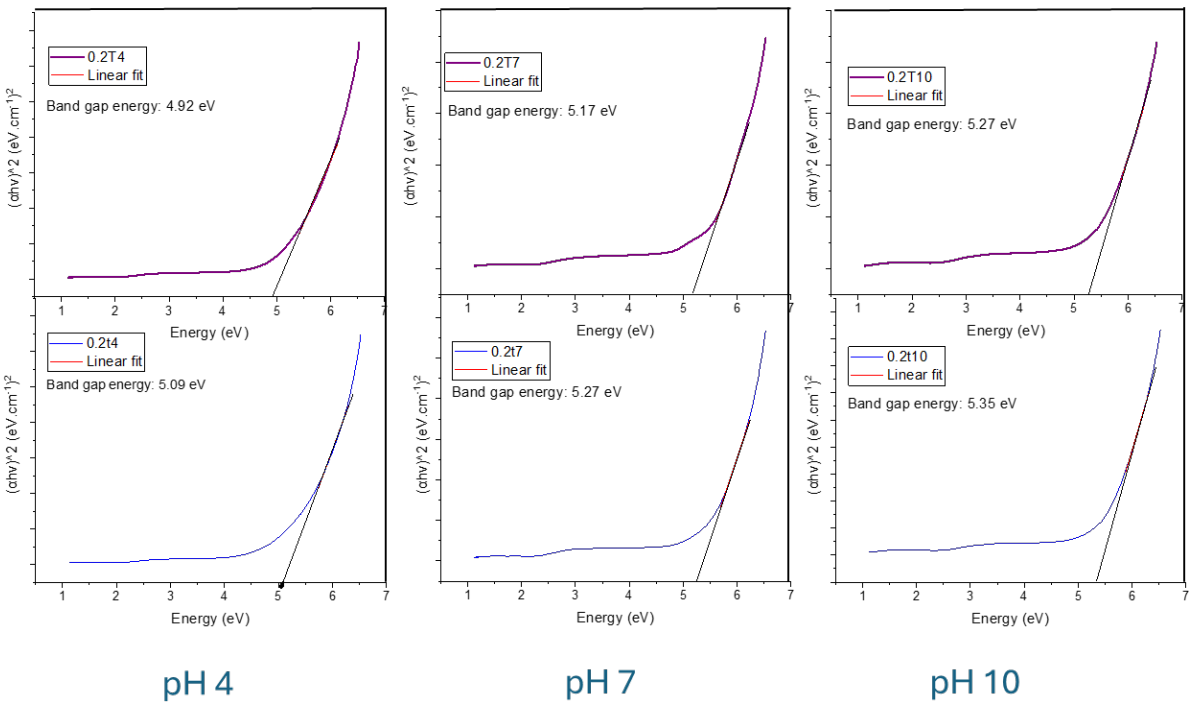

Figure 14: Tauc plots of varying thickness

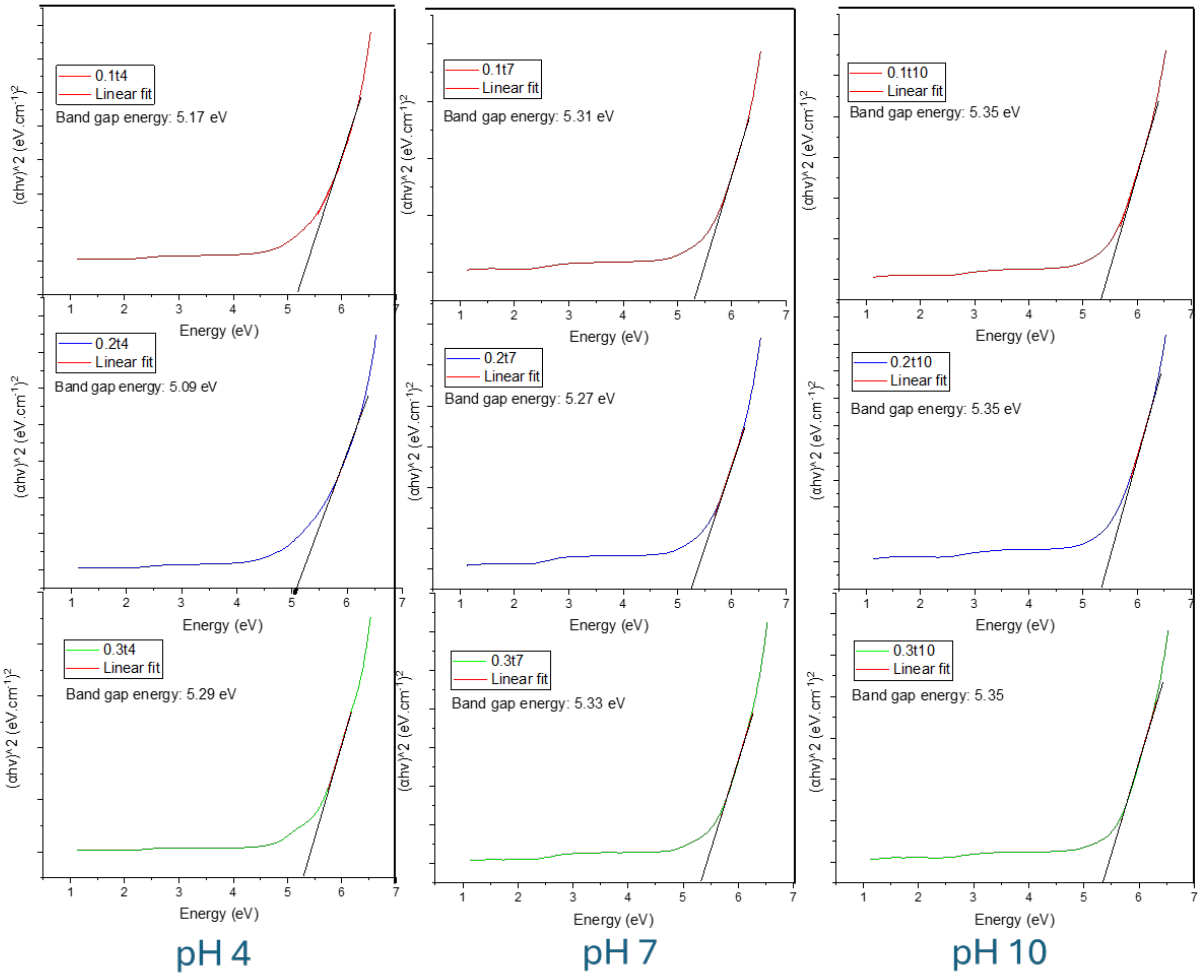

Figure 15: Tauc plots of varying reaction ratio

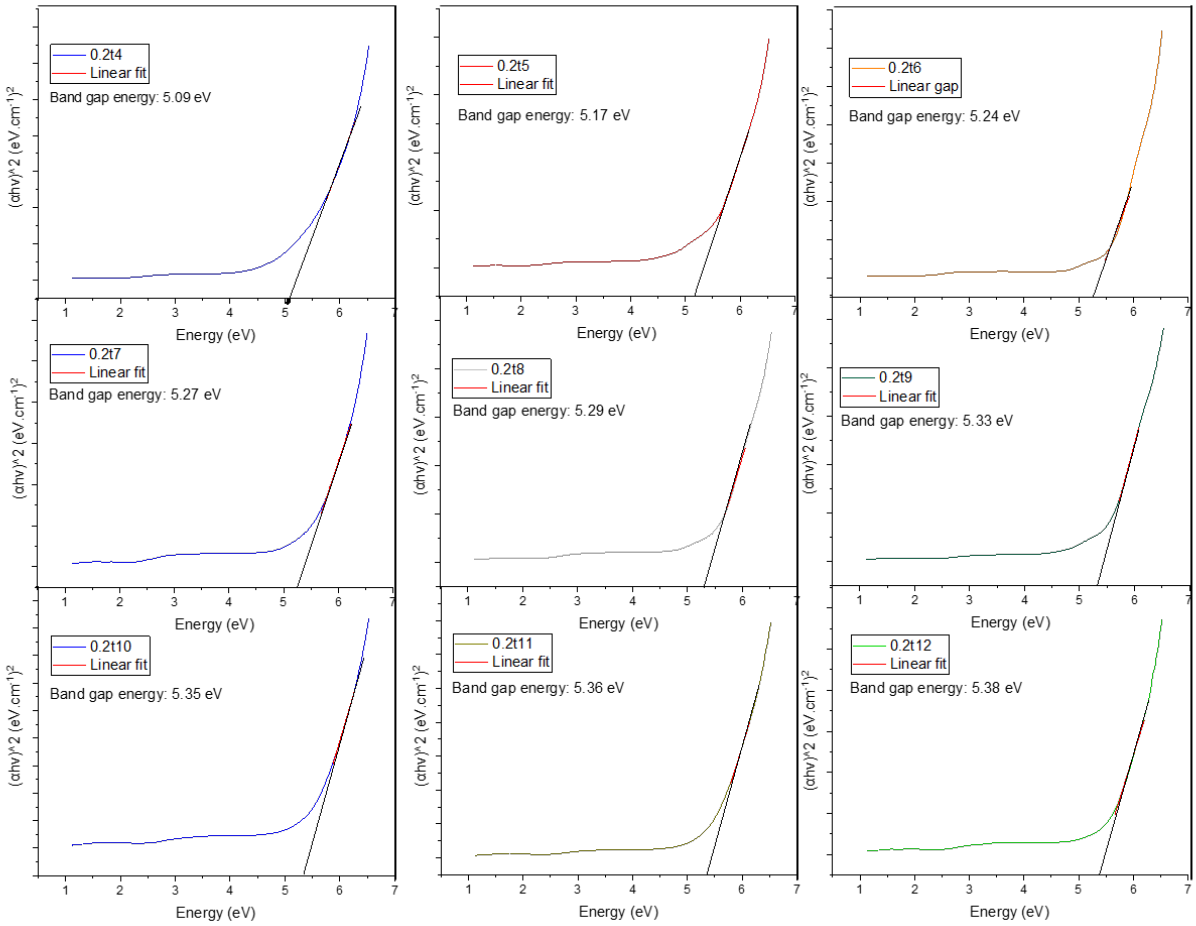

Figure 16: Tauc plots of varying pH

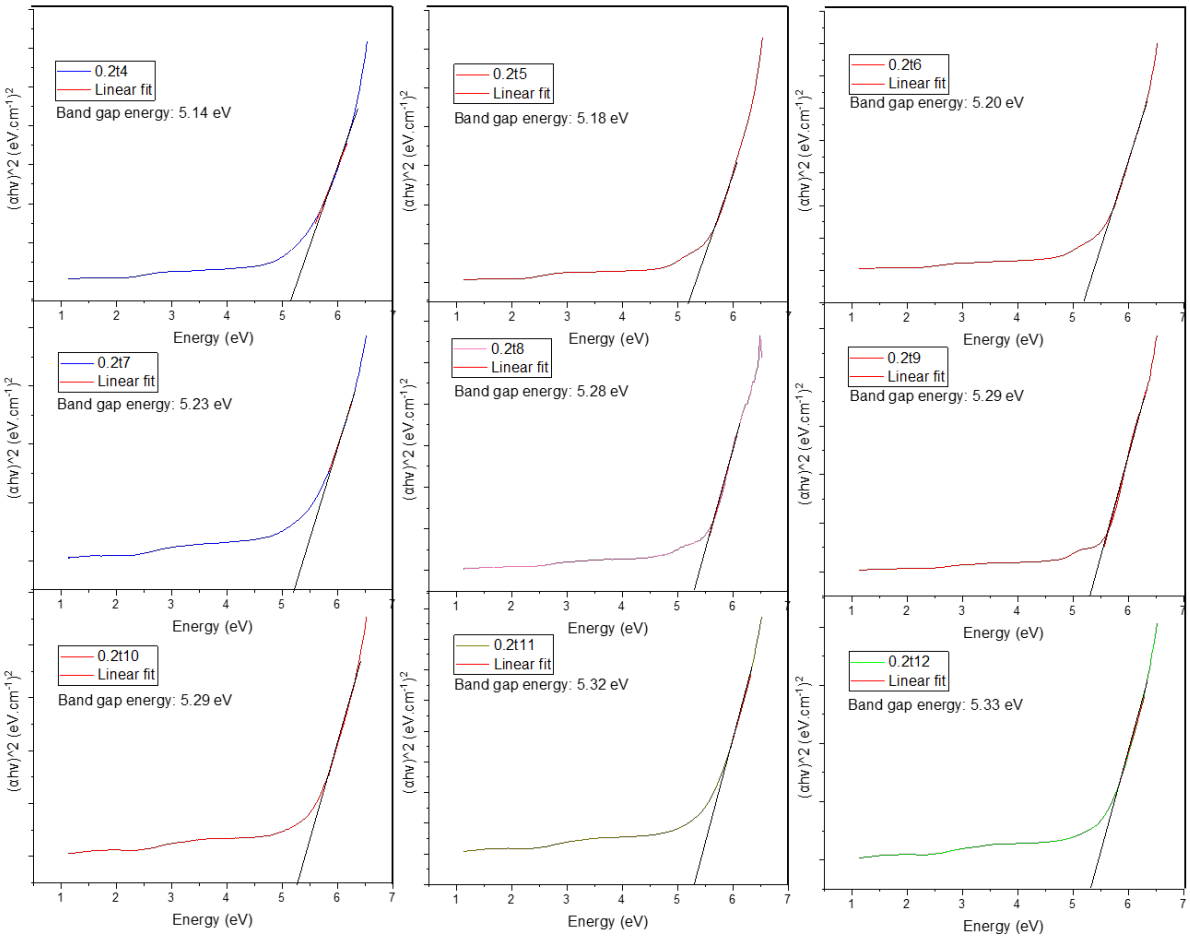

Figure 17: Tauc plots of varying pH with long-term submerging

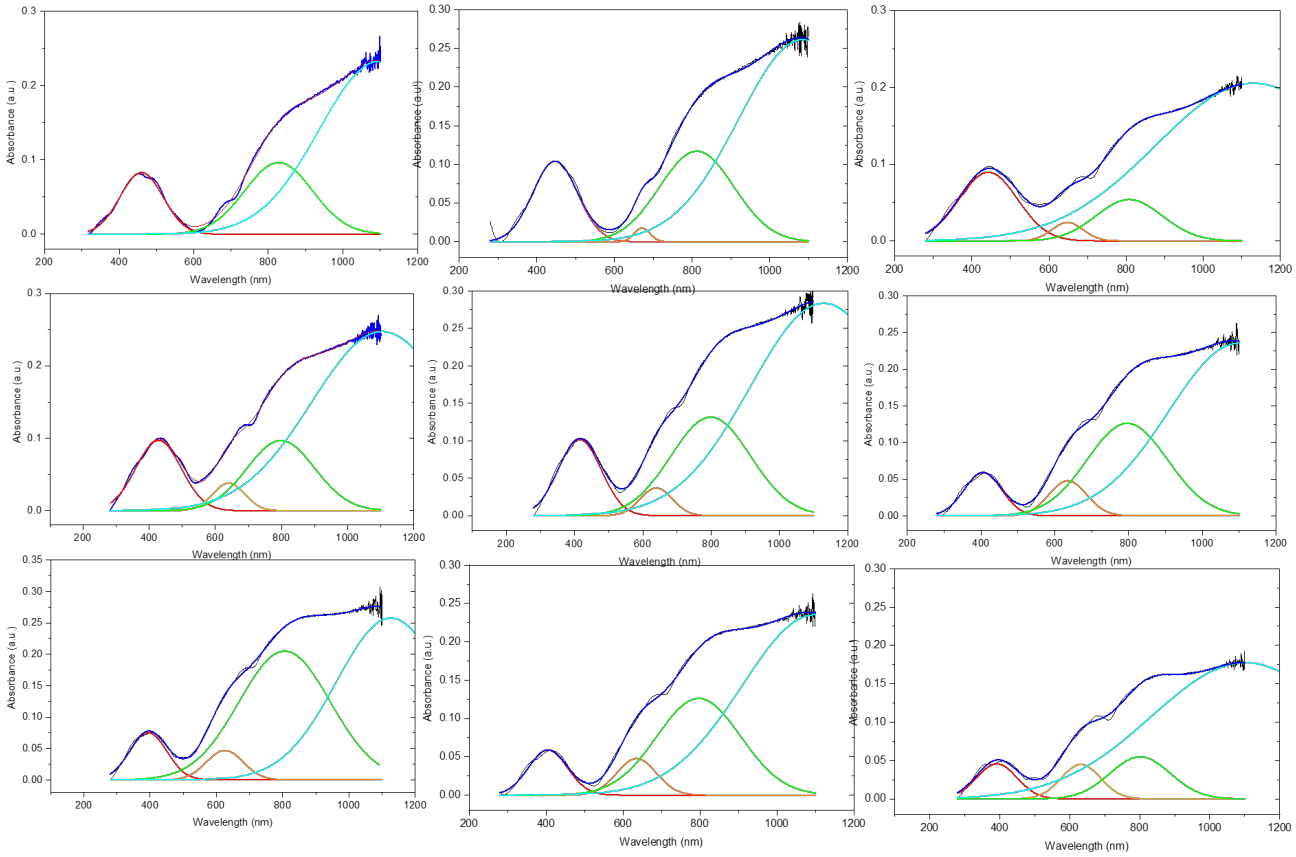

Figure 18: Deconvoluted data of pH 4-12